UDC 669.1.017 DOI: 10.17580/cisisr.2018.02.07

ASSESSMENT AND INTERPRETATION OF NONMETALLIC INCLUSIONS IN STEEL

A. A. Kazakov[1], A. I. Zhitenev[1]

[1] *Peter the Great St. Petersburg Polytechnic University (St. Petersburg, Russia)*

E-mail: kazakov@thixomet.ru

AUTHOR'S INFO

A. A. Kazakov, Dr. Eng., Prof.
A. I. Zhitenev, Engineer

Key words:

non-metallic inclusions, assessment, SEM-EDS method, automated Feature Analysis, cluster analysis, interpretation, thermodynamic simulation, liquid and solidifying steel, solubility surface diagram, steelmaking technology

ABSTRACT

The critical problems of nonmetallic inclusions in steel could be solved by interdisciplinary knowledge based upon steelmaking theory and practice, quantitative metallography and automated feature analysis based on the SEM-EDS analytical technique. A step-by-step method for interpreting the composition of NMI, determined by the SEM-EDS analytical methods, was developed and the nature of all NMIs has been interpreted using thermodynamic modelling. A technique for processing databases, obtained using an automatic feature analyzer (AFA), has been developed. Cluster analysis allowed generalizing these databases by combining NMIs into clusters according to the principle of similarity of their chemical composition and temperature-time nature, depending on the technology of deoxidation and modification of steel. The composition of inclusions along with a large number of analyzed particles, in combination with the methods of thermodynamic simulation makes it possible to restore the temperature-time nature of inclusions, taking into account the entire variety of associated processes occurring in liquid and solidifying steel. Comparison of the determined compositions of NMIs with the results of thermodynamic simulation makes it possible to establish the nature of each cluster of NMIs, associating it with one or another stage of the ladle treatment, casting or solidification. This information is necessary for the development of technological recommendations aimed at increasing the "cleanliness" of steel by NMIs.

Introduction

Despite the advances in the thermodynamic description of the formation of nonmetallic inclusions (NMIs) in liquid and solidified steel [1–4], simulation of the behavior of NMIs during steel ladle treatment, casting and crystallization is impossible. The interconnected processes of formation of NMIs [5], their growth [6] and removal [7, 8] against the background of the hydrodynamics of the liquid and solidified steel [9], dendritic [10] and macro [11] liquation, formation of various structural zones of the slab [12] are too complicated. It should be noted that each inclusion, at the time of its formation, actually fixes the equilibrium with the melt, achieved in micro volumes, taking into account the entire variety of the above-mentioned thermophysical, physicochemical and hydrodynamic processes occurring at all stages of steelmaking. Therefore, an objective statistically significant estimate of the amount, size and, most importantly, the composition of NMIs in steel, carried out by modern experimental methods [13–17], can become the basis for a detailed interpretation of the technology of its production.

Conventional metallographic methods for assessment of nonmetallic inclusions in steels using a light optical microscope (LOM) make it possible to determine their volume fraction, size and character of mutual arrangement of NMIs using ASTM E 1245. An attempt to classify NMIs by chemical composition was made only in the American ASTM E 45 and Russian GOST 1778-70 test methods; however, in both standards the inclusions are ranked more by visual features than by chemical composition, although the names of the inclusions include their chemical composition, for example, spot and stitched oxides, ductile and brittle silicates, sulfides, nitrides (GOST), sulfides, aluminates, silicates, and globular oxides (ASTM E45). Both classifications are primitive and do not include the wide variety of inclusions formed by modern steelmaking technology. For example, when processing steel with calcium and silicon, inclusions are formed consisting of calcium aluminates of different composition and, accordingly, different aggregate states from completely liquid slag inclusions to semi-solid and solid, including high temperature melted inclusions of calcium hexa-aluminate. Depending on the morphology and size, these NMIs can be formally assigned to different types according to ASTM E 45: B (aluminate type), C (silicate type), D (globular oxide type) or different types according to GOST 1778-70: brittle silicates (BS), ductile silicates (DS), spot oxides (SO), and stitched oxides (SO). These two classifications schemes do not reflect the real compositions of non-metallic inclusions; therefore, they can be used only for acceptance testing of metal products; but, they are unsuitable for understanding the nature of NMIs and they are not suitable for improving the technology of steel production. Moreover, the name of the inclusions in accordance with these classifications often puzzles the steelmaker. For example, it is unclear why for a steel treated with calcium, there are silicate inclusions?

The formation and evolution of NMIs is a complex multi-stage process that continuously proceeds throughout the entire steelmaking technology, from the addition of deoxidizing elements into the melt during the steel ladle treatment and up to casting and solidification. According to the temperature-time nature, the following types of NMIs can be distinguished [18]:

- **Primary (I)** NMIs are formed under isothermal conditions during ladle treatment after addition of deoxidizing elements, when their concentrations exceed equilibrium values.

Table I. **Elements and phase composition of NMIs in line pipe steel (wt.%): 0.1 C–1.5 Mn–0.4 Si–0.02 Al–0.005 S**

Elements m_{Me} (SEM-EDS), wt.%				Oxides in non-metallic inclusions, %			Stoichiometric composition of NMIs
Ca	S	Al	Mg	CaO	MgO	Al_2O_3	$CaO{\cdot}Al_2O_3$
49.5	0.2	47	3.3	42	3	55	

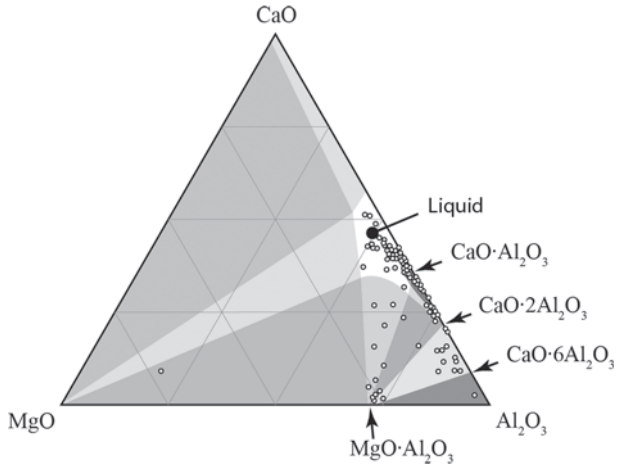

Fig. 1. The phase diagram of the $CaO–MgO–Al_2O_3$ system and the figurative points of the oxide compositions calculated in step 1.

• **Secondary (II)** or pre-crystallization NMIs are formed during cooling from the "steelmaking temperature" to the liquidus temperature, when the solubility of oxygen and deoxidizing elements in the melt is reduced.

• **Tertiary (III)** or crystallization NMIs are formed during the solidification of the steel not only by reducing its temperature, but mainly due to the enrichment of the liquid part of the dendritic cell with segregating impurities. Quaternary NMIs precipitate in solid metal and we do not consider them here.

The study of the real composition of individual NMIs by SEM-EDS microanalysis is a well-established procedure for many years and has been successfully used in research laboratories [4-8, 13, 19], but this information does not provide an objective account of the wide variety of NMIs in actual commercial steels. For an objective statistically significant assessment of the volume fraction, size and composition of NMIs in commercial steels, it is advisable to use databases obtained by the automatic feature analysis (AFA) method that contains information on many NMIs. The number of particles analyzed by AFA must be comparable to the metallographic methods of research using light optical microscopes. The present article is devoted to the development of such methods and to the illustration of the first experience of their use.

Method for Interpretation of Nonmetallic Inclusions

Step-by-Step Method for Interpretation of Individual Nonmetallic Inclusions in Steel

The chemical composition of NMIs in steel is usually determined using an SEM equipped with an energy-dispersive spectrometer (EDS) for chemical analysis. This method makes it possible to estimate the approximate elemental composition of NMI in wt.%, but the uncertainty of the stoichiometric composition of the oxide found does not allow us to make a judgment about its compound nature and, therefore, offer possible options for controlling the origin of these inclusions. To answer these questions, we developed a step-by-step method for further processing of data obtained by the SEM-EDS method.

Step 1. Calculation of the Stoichiometric Composition of Oxides According to the Elemental Composition of the NMIs

If Ca and S were found in the complex oxy-sulfide NMIs, to calculate Ca in the oxides ($m_{Ca'}$) we have to extract Ca fixed as CaS from the total Ca (m_{Ca}) in the NMIs: $m_{Ca'} = m_{Ca} - \frac{A_{Ca} \cdot m_S}{A_S}$. Here and below A_j is the atomic weight of elements (j = Ca, S, O, Me). Now, we can calculate the content of each of the oxides, knowing their composition (x, y) and the concentration of the deoxidizer (m_{Me}): $m_{Me_xO_y} = m_{Me} \cdot \left(1 + \frac{y \cdot A_0}{x \cdot A_{Me}}\right)$, from which we find the stoichiometric composition of the complex oxide: $Me_xO_y, \% = \frac{m_{Me_xO_y} \cdot 100\%}{\sum_i \left(m_{Me_xO_y\,i}\right)}$.

An example of such a calculation is given in **Table 1.**

Step 2. Improvement of the Stoichiometric Composition of Oxides Based on the Phase Diagram

All the points corresponding to the oxide compositions found among all the investigated NMIs were placed on the corresponding phase diagram (**Fig. 1**), constructed for a temperature close to the temperature of the steelmaking processes (1550 °C). If these points fall into the region of the same stoichiometric compositions that were found in the previous step, no adjustment is required. If the points have appeared in other phase regions, for example, in the field of liquid slag, such compositions of NMIs should be adjusted in accordance with their position on the phase diagram of the corresponding oxide system (Fig. 1).

Step 3. Evaluation of Residual Concentrations of Elements in the Steel Melt, from which the Oxides with Compositions Found in Step №2 are Formed

Here is a solution for the inverse task: by means of a Solubility Surface Diagram (SSD), we define the residual concentrations of elements in liquid steel from which the NMIs with the composition found in the previous step were formed. To do this, it is necessary to arrange an SSD on the region of existence where this oxide will be observed (**Fig. 2**). The range of concentration changes for the deoxidizing elements, found from the SSD, at which the desired oxide is formed, will be used in the next step of the interpretation.

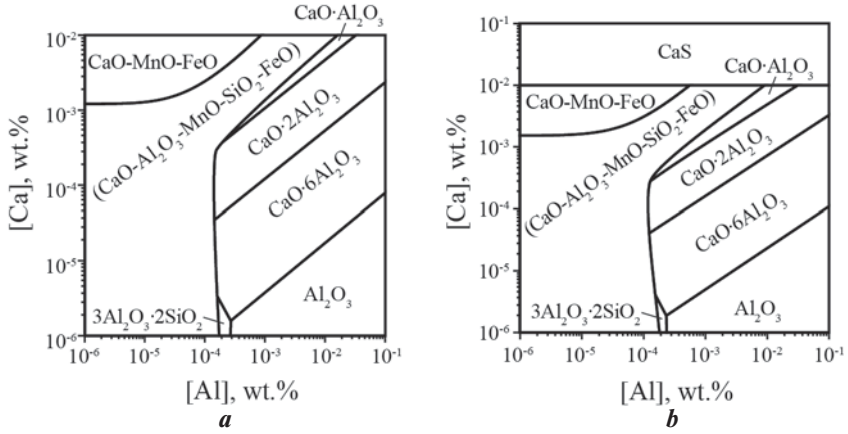

Fig. 2. SSDs for the systems being investigated to find the composition of the melt from which the oxide with the composition found in step 2 is formed *a* —1580 °C; *b* — 1500 °C

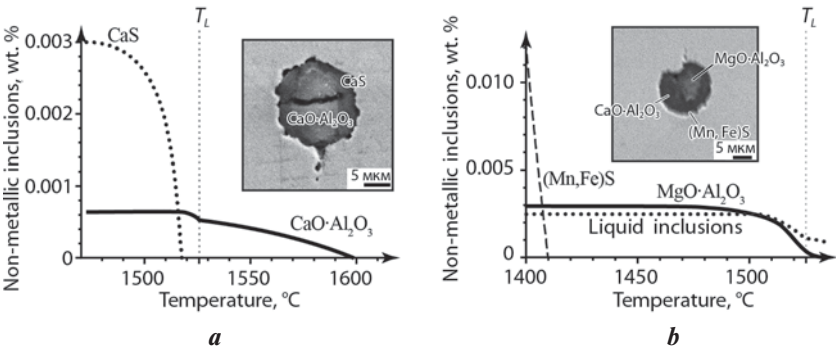

Fig. 3. NMIs and the results of simulation the processes of their formation in liquid and solidifying steel, (wt.%):
a — [C] = 0.07; [Si] = 0.25; [Mn] = 1.3; [Al] = 0.02; [Ca] = 0.012; [S] = 0.005;
b — [C] = 0.09; [Si] = 0.25; [Mn] = 1.7; [Al] = 0.04; [Ca] = 0.0005; [Mg] = 0.0001; [S] = 0.003

Step 4. Revealing the Thermal Nature of NMIs Based on the Composition of the Steel Found in Step № 3

To simulate NMI formation in the liquid and solidified steel, we set the concentrations of the deoxidizing elements from the range that was found in step № 3. Then, by varying the concentrations within this range, we can restore the nature of the NMIs, whose composition was found in step 1 and improved in step 2 (Fig. 1). An example of such a simulation is shown in **Fig. 3, *a***: on the secondary calcium aluminates, as on the substrate, tertiary calcium sulfides were formed. It is this arrangement of the compounds that we see in the image of the NMI in the SEM: the $CaO{\cdot}Al_2O_3$ inclusion core formed in the liquid steel is coated with CaS formed in the solidifying metal. Here, calcium was sufficient to react with sulfur during solidification after the formation of $CaO{\cdot}Al_2O_3$ in liquid steel.

In **Fig. 3, *b***, another example is given where, in conditions of a calcium deficiency in liquid steel, a liquid slag based on $CaO{\cdot}Al_2O_3$ and a solid magnesium spinel $MgO{\cdot}Al_2O_3$ are formed simultaneously. During steel solidification there was no calcium left in the melt, so a tertiary sulfide MnS–FeS was formed on the surface of these secondary oxides. This sulfide is seen as a light rim on the rounded surface of the oxides.

Let us consider other more complicated simulation examples for the interpretation of multiphase inclusions formed in steels with different compositions (**Fig. 4**). It follows from Fig. 4, *b* that first in the melt primary and secondary liquid oxy-sulfide inclusions and solid magnesia spinel are formed. With further cooling of the liquid steel and its solidification, liquid primary and secondary oxy-sulfide inclusions crystallize (Fig. 4, *c*). We note that, in the example considered, the complex multiphase inclusion has rounded but irregular shapes (Fig. 4, *a*), because when formed it was semi-solid, consisting of approximately equal parts of liquid oxy-sulfides and solid magnesium spinel (Fig. 4, *b*). Simulation results of formation processes of primary and secondary liquid, as well as secondary solid calcium aluminates in steel with a different composition, are shown in Figs. 4, *d* – 4, *f*.

From a comparison of the results in Fig. 4, it follows that all compounds detected in the investigation of NMIs by SEM-EDS analysis have been interpreted by thermodynamic simulation. Note that in the example in Fig. 4, *d* — 4, *f*, the inclusion has the shape of a regular sphere (Fig. 4, *d*) because it has been formed from mainly liquid oxy-sulfide slag (Fig. 4, *e*), in which all the oxides of various composition and calcium sulfides crystallized sequentially and were found experimentally and by simulation (Fig. 4, *f*).

Cluster Analysis of the Automatic Feature Analysis Data

Automatic feature analysis (AFA), realized by the SEM-EDS analytical method for inclusions in steel, allows an objective assessment of their composition, while the study of a large number of particles, comparable to that usually studied by LOM, makes it possible to obtain reliable information not only about their quantity and size, but also the elemental composition of each of the detected inclusions [20, 21]. However, these data are rather complicated and require the appropriate clustering of the inclusions into groups. The AFA software does not perform interpretation of the results. In the present work, clustering was carried out by the k-means method [22], combining the NMIs by the similarity of their chemical composition. Clustering is the dividing of a set of objects into non-overlapping subsets (clusters), so that each cluster contains similar objects, and the objects of

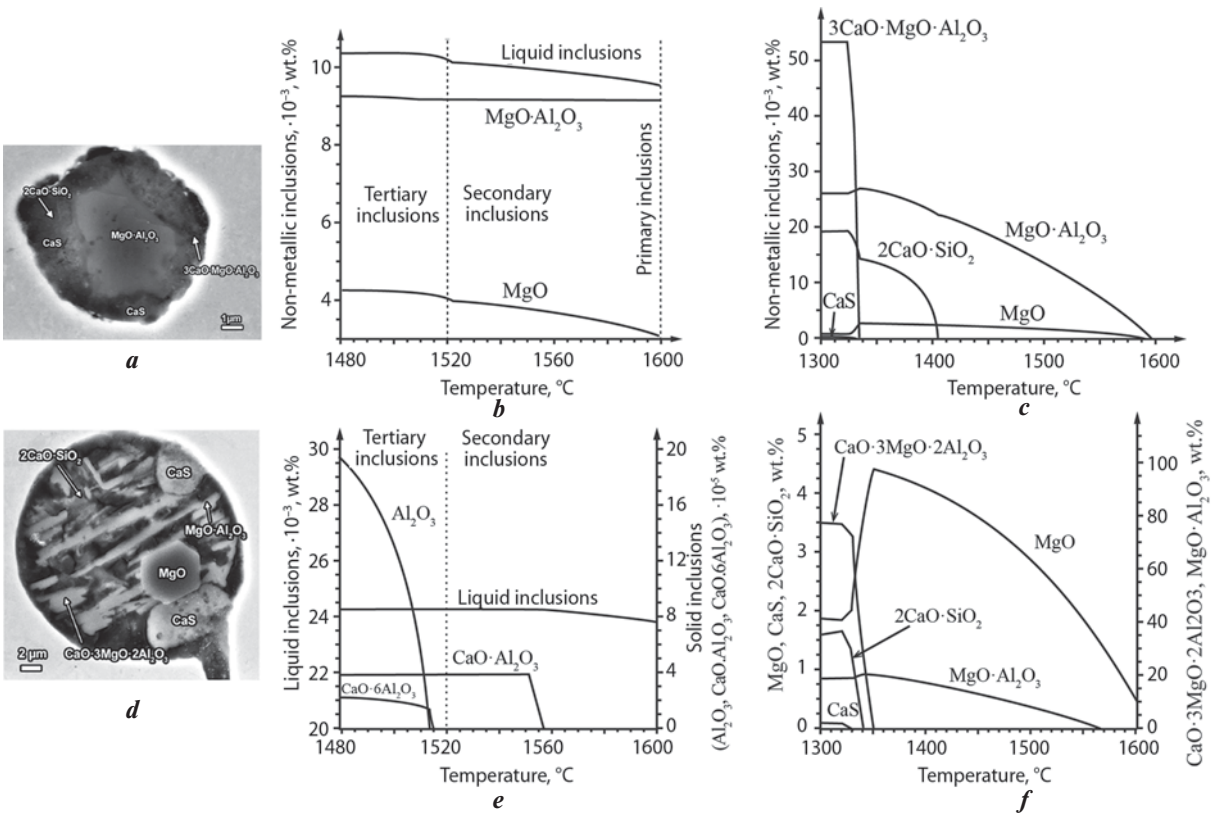

Fig. 4. NMIs (*a, d*) and the results of simulation the processes of their formation in liquid and solidifying steel (*b, e*), including crystallization of primary and secondary liquid oxy-sulfide inclusions (*c, f*), wt.%:
b — [Mg] = 0.005; [Ca] = 0.0026; [Al] = 0.02; *c* — CaO ≈ 42; MgO ≈ 28; Al_2O_3 ≈ 23; SiO_2 ≈ 6; CaS ≈ 0.12; *e* — [Mg] = 10^{-6}; [Ca] = 0.007; [Al] = 0.02; *f* — Al_2O_3 ≈ 25; CaO ≈ 35; MgO ≈ 32; SiO_2 ≈ 7; CaS ≈ 0.05

different clusters differ from each other. This approach adequately estimates the main groups of NMIs, typical for the investigated specimen.

An important clustering problem is the choice of a finite number of groups into which nonmetallic inclusions are divided. Minimally this is one group, which includes all the inclusions found; the maximum is the number of all detected NMIs types. The number of groups was chosen in accordance with the change in the distortion value, which was calculated as the sum of the mean square Euclidean distances between the point vector and the center of the cluster to which it belongs. As the number of clusters increases, the distortion decreases. The choice of the number of groups was carried out based on an analysis of the dependence of the distortion on the number of groups and their component composition. The separation of inclusions into groups was completed when it does not lead to the appearance of clusters that differ markedly in composition. The method was tested on a specimen of wheel steel, cut from the transverse template of a continuously cast round section with a diameter 430 mm. To estimate the variety of nonmetallic inclusions remaining in the billet, the specimen was cut from its central region with the highest concentration of nonmetallic inclusions [23]. Fig. 5, *a* gives an example of the simulation process for formation of NMIs in the wheel steel.

After setting the total oxygen content, found experimentally, as the initial [O] = 25 ppm, we get the simulation results **(Fig. 5, *a*)**. In the liquid steel at 1550 °C, the primary NMIs are formed, and with subsequent cooling of the melt, the secondary NMIs are formed. Along with Al_2O_3, liquid oxy-sulfide inclusions and a small amount of calcium hexa-aluminates are formed, from which, when cooled below 1550 °C, solid oxides and sulfides precipitate. These exact complex multiphase inclusions, combined into the clusters, have been found in investigated specimen **(fig. 5, *b*)**.

All the compositions of NMIs found in steel and depicted in Al–Mn–S coordinates (Fig. 5, *b*) line up connecting the angle "Al" with the point corresponding to manganese sulfide on the Mn–S axis. Evolution of the composition with a decrease in the start temperature of NMIs formation proceeds from the primary (I) and secondary (II) NMIs of Al–Mn–Si–S–Ca cluster in liquid steel to the Mn–S–Al–N–Ti cluster (III) in the first half of the solidification and, finally, to the inclusions (III) of the Mn–S–Al–Ti–N + N–Ti–V–Mn–S system in the second half of the steel solidification (Fig. 5, *b*).

Conclusions

The imperfection of Russian and International standards for estimation of the NMIs composition in modern steels was shown. A step-by-step method for interpreting the composition of individual NMIs, determined by the SEM-EDS analytical methods, was developed.

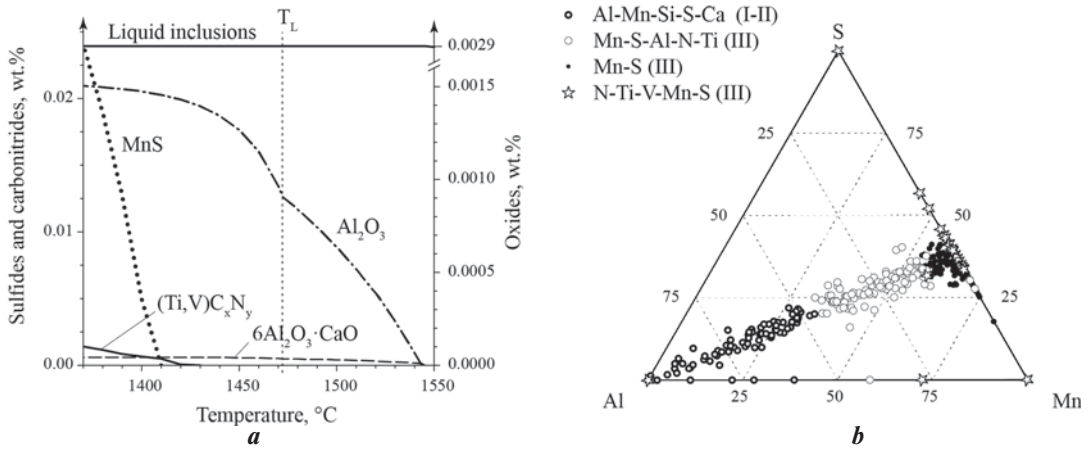

Fig. 5. Interpretation of NMIs in wheel steel (wt.%):
[C] = 0.68, [Si] = 0.4, [Mn] = 0.9; [Al] = 0.004, [Ca] = 0.0005, [Ti] = 0.003, [S] = 0.019; [O] = 25 ppm, and [N] = 40 ppm;
a — thermodynamic simulation of NMI formation in wheel steel; *b* — clusters of non-metallic inclusions and their evolution in liquid and solidifying steel

Examples of such an interpretation are given for both simple two-phase and complex multiphase inclusions found in commercial steels. The nature of all NMIs detected by SEM-EDS microanalysis has been interpreted using thermodynamic modeling.

A technique for processing databases obtained using an automatic feature analyzer (AFA) has been developed. Cluster analysis allowed generalizing these databases by combining NMIs into clusters according to the principle of similarity of their chemical composition and temperature-time nature, depending on the technology of deoxidation and modification of steel. Comparison of the determined compositions of NMIs with the results of thermodynamic simulation makes it possible to establish the nature of each cluster of NMIs, associating it with one or another stage of the ladle treatment, casting or solidification. This information is necessary for the development of technological recommendations aimed at increasing the "cleanliness" of steel by NMIs. The composition of inclusions along with many analyzed particles in combination with the methods of thermodynamic simulation makes it possible to restore the temperature-time nature of inclusions, considering the entire variety of associated thermophysical, hydrodynamic and physicochemical processes occurring in liquid and solidifying steel.

REFERENCES

1. You D., Michelic S., Presoly P., Liu J., Bernhard C. Modeling Inclusion Formation during Solidification of Steel: A Review. *Metals,* 2017. Vol. 7 (October). pp. 1–31.
2. Hack K. Inclusion Cleanness in Calcium-Treated Steel Grades. *The SGTE Casebook: Thermodynamics at Work, Second Edition*. Woodhead Publishing Limited, Cambridge, England. 2008, pp. 267–272.
3. Costa-e-Silva A. Applications of Multicomponent Databases to the Improvement of Steel Processing and Design. *Journal of Phase Equilibria and Diffusion,* 2017. Vol. 38. No. 6 (December). pp. 916–927.
4. Kong L., Deng Z., Zhu M. Formation and Evolution of Non-metallic Inclusions in Medium Mn Steel during Secondary Refining Process. *ISIJ International*. 2017. Vol. 57. No. 9 (July 2017). pp. 1537–1545.
5. Zhang L. Nucleation and Growth of Alumina Inclusions during Steel Deoxidation. *85th Steelmaking Conference Proceedings, Nashville, TN*. 2002. Vol. 85 (March). pp. 463–476.
6. Zhang L. Nucleation, Growth, Transport and Entrapment of Inclusions during Steel Casting. *JOM*. 2013. Vol. 65. No. 9. pp. 1138–1144.
7. Reis B. H., Bielefeldt W. V., Vilela A. C. F. Efficiency of Inclusion Absorption by Slags during Secondary Refining of Steel. *ISIJ International*. 2014. Vol. 54. No. 7 (August). pp. 1584–1591.
8. Kalisz D. Interaction of Non-Metallic Inclusion Particles With Advancing Solidification Front. *Archives of Metallurgy And Materials*. 2014. Vol. 59. Issue 2 (June). pp. 493–500.
9. Banaszek J., Mcfadden S., Browne, D. J., Sturz L., Zimmermann G. Natural Convection and Columnar-to-Equiaxed Transition Prediction in a Front-Tracking Model of Alloy Solidification. *Metallurgical and Materials Transactions: A*. 2007. Vol. 38A., No. 7. (July). pp. 1476–1484.
10. Matsumiya T., Yamada W., Koseki T., Ueshama Y. Mathematical Analysis of Segregation and Compositional Changes of Nonmetallic Inclusions in Steel during Solidification. *Nippon Steel Technical Report*. 1993. No. 57 (April). pp. 50–56.
11. Pikkarainen T., Vuorenmaa V., Rentola I., Leinonen M. and Porter D. Effect of Superheat on Macrostructure and Macrosegregation in Continuous Cast Low-Alloy Steel Slabs. *IOP Conference Series: Material Science and Engineering*. Vol. 117. pp. 1–7.
12. Wang C. Y., Beckermann C. Prediction of Columnar to Equiaxed Transition during Diffusion-Controlled Dendritic Alloy Solidification. *Metallurgical and Materials Transactions A*. 1994. Vol. 25A. No. 5 (May). pp. 1081–1093.
13. Kazakov A., Kovalev P., Ryaboshchuk S., Mileikovsky A., Malakhov N. Study of Thermal Time Nature of Non-Metallic Inclusions in Order to Improve Metallurgical Quality of High-Strength Tube Steels. *Chernye Metally (Ferrous metals)*. 2009. No. 12. pp. 5–11.
14. Kazakov A. Nonmetallic Inclusions in Steel – Origin, Estimation, Interpretation and Control. *Microscopy and Microanalysis*. 2016. Vol. 22. No. S3 (July). pp. 1938–1939.
15. Kazakov A., Zhitenev A., Ryaboshuk S. Interpretation and Classification of Non-Metallic Inclusions. *Materials Performance and Characterization*. 2016. Vol. 5, No. 5 (December). pp. 535–543.
16. Kazakov A. A., Lubochko D. A., Ryabochuk S. B., Chigintsev L. S. Investigation of the Nature of Nonmetallic Inclusions in HSLA Steels Using an Automatic Particle Analyzer. *Chernye Metally*. 2014. No. 4. pp. 85–90.

17. Kazakov A. A., Kovalev P. V., Ryaboshuk S. V., Zhironkin M. V., Krasnov A.V. Control of Nonmetallic Inclusions Formation during Converter Steel Production. *Chernye Metally*. 2014. No. 4. pp. 91–96.
18. Yavoyskiy V. I., Bliznyukov S.A., Vishkarev A. F., Gorokhov L. S., Khokhlov S. F., Yavoyskiy A. V. Deoxidation of Steel, Nucleation, Formation, Coalescence and Removal of Nonmetallic Inclusions. Inclusions and Gases in Steels, Moscow. Metallurgiya. 1979. pp. 57–61.
19. Kiessling R., Lange N. Inclusions belonging to the pseudoternary system $MnO–SiO_2–Al_2O_3$ and related system. Nonmetallic Inclusions in Steel. Iron and Steel Institute. London. 1965, pp. 10–17.
20. Story S. R., Smith S. M., Fruehan R. J., Casuccio G. S., Potter M. S., Lersch T. L. Application of Rapid Inclusion Identification and Analysis. *Iron & Steel Technology*. 2005. Vol. 2. No. 9. pp. 41–49.
21. Ren Y., Wang Y., Li S., Zhang L., Zuo X., Lekahn S., Peaslee K. Detection of Non-metallic Inclusions in Steel Continuous Casting Billets. *Metallurgical and Materials Transactions*. 2014. Vol. 45. No. 4 (August). pp. 1291–1303.
22. Jain A. K., Murty M. N., Flynn P. J. Data Clustering: A Review. *ACM Computing Surveys*. 1999. Vol. 31. No. 3 (September). pp. 264–323.
23. Kazakov A., Zhitenev A., Kovalev P. Distribution Pattern of Nonmetallic Inclusions on a Cross Section of Continuous Cast Steel Billets For Rails. *Microscopy and Microanalysis*. 2015. Vol. 21. No. S3 (August). pp. 1751–1752.

UDC 621.77.014 DOI: 10.17580/cisisr.2018.02.08

EVOLUTION OF CEMENTITE IN PEARLITE CARBON STEEL WIRE AT COMBINED DEFORMATIONAL PROCESSING*

M. A. Polyakova[1], K. Narasimhan[2], M. J. N. V. Prasad[2], Yu. Yu. Efimova[1]

[1] *Nosov Magnitogorsk State Technical University (Magnitogorsk, Russia)*
[2] *Indian Institute of Technology Bombay (Mumbai, India)*

E-mail: m.polyakova@magtu.ru, nara@iitb.ac.in, yu.efimova@magtu.ru

AUTHOR'S INFO

M. A. Polyakova, Dr. Eng., Prof., Dept. of Material Processing,
K. Narasimhan, Dr. Eng. Department of Metallurgical Engineering and Materials Science,
M. J. N. V. Prasad, Dr. Eng. Department of Metallurgical Engineering and Materials Science,
Yu. Yu. Efimova, Cand. Eng., Associate Prof., Dept. of Material Processing

Key words:

Keywords: carbon steel wire; cementite; pearlite; combined deformational processing; drawing; bending; torsion.

ABSTRACT

Implementation of combined methods of deformational processing is on the cutting-edge of downstream steel manufacturing. The effect of plastic deformation on metals is the irreversible particular changes in microstructure. To develop new technological processes of metal ware manufacturing it is necessary to study the microstructure changing features in steel in order to predict its properties. Carbon steel wire with pearlite structure is used for a wide range of engineering components. Carbon steel wire was plastically deformed by drawing in combination with bending and torsion. Such combination resulted in characteristic changing of cementite plates. The main objective of the paper is to correlate cementite evolution of carbon steel wire after combined deformational processing by drawing with bending and torsion with its mechanical properties. The construction of the used laboratory setup consisted of two drawing dies and four-rolls system which makes it possible to change the deformation degree during drawing, bending by the use of rolls with different diameters as well as torsion deformation in wide range. Scanning electron microscopy and tensile test were used for analysis of processed carbon steel wire. It was observed that after combined deformational processing cementite lamellas were destroyed. After combination of drawing with bending, cementite lamellas became curve especially when in the four-rolls system the rolls with smaller diameter were installed. By the combination of drawing with bending and torsion, the cementite lamellas changed in the same manner as without torsion deformation, but boundaries between pearlite colonies could not be identified with smaller diameter of rolls. Because combined deformation schemes during combination of different kinds of deformation was rather complicated, they had different impact on strength and ductile properties of the processed pearlitic wire.

1. Introduction

Pearlitic steel wire has a wide range of application. It is used as semi-product in downstream steel manufacturing for cables, meshes, cord, etc. and as a finished product in electronic devices, medical equipment, watches, etc. [1]. Pearlite structure consists of cementite lamellae with low extent of ferrite which are very sensitive to any kind of deformational processing. This peculiarity of pearlite change on each stage of wire production, influences the behavior of eutectoid steel at further stages of downstream production [2–4].

The basic operation for steel wire production is drawing. The main strain at drawing is the tensile deformation along the wire axis. This feature of the applied strain affects the changes in microstructure of the processed wire when steel grains elongate along the drawing direction. Such kind of microstructure is denoted as texture which affects to high extent on mechanical properties of drawn pearlitic steel wire. Much research has focused on texture formation after drawing and its effect on mechanical properties of pearlitic wire [5–10]. It was proved

* Authors appreciate PhD Alexandr Gulin (Nosov Magnitogorsk state technical university) for conducting tensile tests of the processed carbon steel wire and interpreting the experimental results.